Distinct bile salt hydrolase substrate preferences dictate *C. difficile* pathogenesis

One sentence summary: Bile salt hydrolase activity inhibits *C. difficile* by shaping the conventional and non-canonical conjugated bile acid pools

Matthew H. Foley[1,2]†, Morgan E. Walker[3]†, Allison K. Stewart[4], Sarah O'Flaherty[2], Emily C. Gentry[5,6], Garrison Allen[1], Shakshi Patel[3], Meichen Pan[2], Violet V. Beaty[3], Molly E. Vanhoy[1], Michael K. Dougherty[7], Sarah K. McGill[7], Ajay Gulati[7,8], Pieter C. Dorrestein[5,6], Erin S. Baker[4], Matthew R. Redinbo[3,9]*, Rodolphe Barrangou[2]*, Casey M. Theriot[1]*.

1. Department of Pathobiology and Population Health, College of Veterinary Medicine, North Carolina State University, Raleigh, NC, USA.

2. Department of Food, Bioprocessing and Nutrition Sciences, North Carolina State University, Raleigh, NC, USA.

3. Department of Chemistry, University of North Carolina at Chapel Hill, Chapel Hill, NC, USA.

4. Department of Chemistry, North Carolina State University, Raleigh, NC, USA

5. Skaggs School of Pharmacy and Pharmaceutical Sciences, University of California San Diego, La Jolla, San Diego, CA, USA

6. Collaborative Mass Spectrometry Innovation Center, Skaggs School of Pharmacy and Pharmaceutical Sciences, University of California San Diego, La Jolla, CA, USA

7. Department of Medicine, Division of Gastroenterology and Hepatology, University of North Carolina at Chapel Hill, Chapel Hill, NC, USA

8. Department of Pathology and Laboratory Medicine, University of North Carolina at Chapel Hill, Chapel Hill, NC, USA

24 9. Departments of Biochemistry & Biophysics, and Microbiology & Immunology, and the
25 Integrated Program in Biological and Genome Sciences, University of North Carolina at Chapel
26 Hill, Chapel Hill, NC, USA
27
28 † Authors contributed equally to this work
29 * Corresponding Authors Matthew R. Redinbo redinbo@unc.edu; Rodolphe Barrangou,
30 rbarran@ncsu.edu; Casey M. Theriot, cmtherio@ncsu.edu
31
32 **Classification**
33 Biological Sciences, Microbiology.
34
35 **Keywords**
36 bile salt hydrolase, bile acid, live biotherapeutic, *Lactobacillus*, *Clostridioides difficile*

Summary paragraph: Bile acids (BAs) mediate the crosstalk between human and microbial cells and influence intestinal diseases including *Clostridioides difficile* infection (CDI). While bile salt hydrolases (BSHs) shape the BA pool by deconjugating conjugated BAs, the basis for their substrate preferences and impact on *C. difficile* remain elusive. Here, we survey the diversity of *Lactobacillus* BSHs and unravel the structural basis of their substrate preference. We show that leveraging BSH activity and specificity is an effective strategy to prevent *C. difficile* growth in clinically relevant CDI models. A range of non-canonical conjugated BAs is also identified, comprising unique BSH substrates that also inhibit *C. difficile* spore germination. These findings establish BSHs as intestinal enzymes essential to BA homeostasis and colonization resistance against *C. difficile*.

47 **Introduction**

48 Bile acids (BAs) are host-synthesized and microbial-derived metabolites that
49 support intestinal health and homeostasis by providing a scaffold for host-microbiome crosstalk
50 and adaptation (*1, 2*). Host-encoded BA receptors recognize BAs as signaling molecules to
51 regulate key aspects of host immunity (*3*), metabolism (*4*), and circadian rhythms (*5, 6*). BAs
52 also shape the microbiota, with specific taxa being inherently more resistant to bile stress by
53 harboring mechanisms to survive BA exposure (*7, 8*). The influence of BAs on the microbiota
54 composition is reciprocated by the microbial transformation of BAs to unlock the chemical
55 complexity present in the intestinal BA pool (*9*). The resulting mosaicism of the BA pool is a
56 hallmark of host health and is dependent on the collective activity of microbiome-encoded BA
57 altering enzymes (*10*).

58 One such enzyme, bile salt hydrolase (BSH), comprises a family of microbial
59 enzymes that catalyze a critical step in BA biosynthesis (*11*). Primary conjugated BAs
60 synthesized in the liver, such as the tauro- and glyco- conjugates of cholic acid (TCA, GCA), are
61 deconjugated by BSHs to generate cholic acid (CA) (**Fig. 1A**; BA names and abbreviations are
62 summarized in **Fig. S1**). This vanguard catalytic step acts as a "gatekeeper'' for subsequent BA
63 transformations that turn primary BAs into secondary BAs (i.e. deoxycholic acid -DCA- formed
64 from the 7α-dehydroxylation of CA) (*1, 11*).

65 Dysregulation of BA biosynthesis and BSH activity has been directly implicated in obesity (*12*),
66 cancer (*13*), inflammatory bowel disease (*3*), and colonization resistance against pathogens
67 including *Clostridioides difficile* (*14, 15*). Strategically managing BSH activity to rationally
68 toggle BA metabolism and judiciously alter intestinal pathobiology presents an emerging
69 therapeutic approach. Additionally, the recent discovery of non-canonical conjugated BAs has

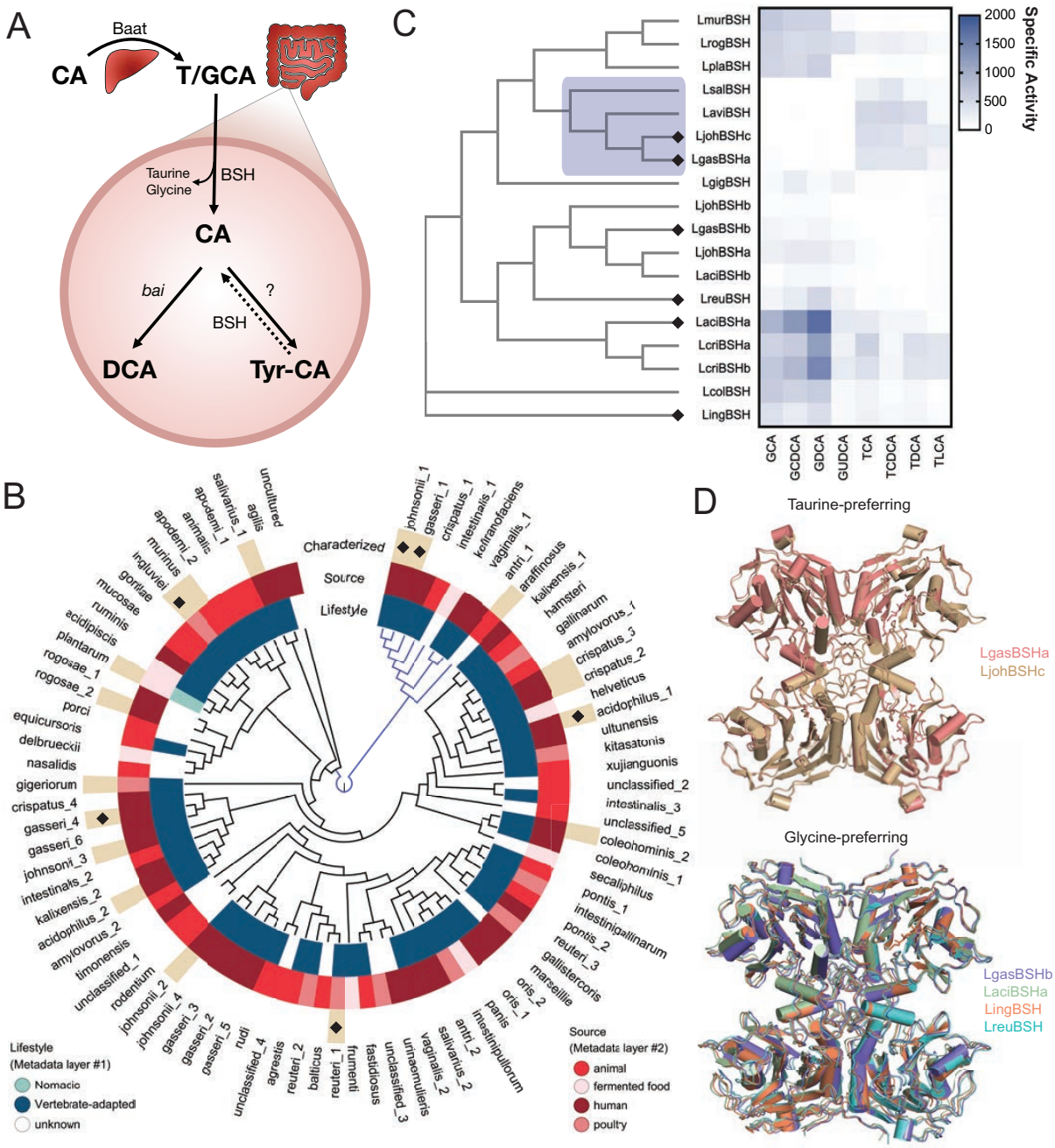

Figure 1.

considerably increased the complexity of the BA pool and altered the paradigm of BSH-BA biology. In particular, BSHs do not appear to process these non-canonical conjugated BAs *in vitro*, indicating that renewed and expanded investigations of BSH-substrate relationships are warranted (**Fig. 1A)** (*16-18*).

76 Here, we examine the phylogenetic, biochemical, structural diversity and
77 specificity of BSHs in *Lactobacillus*, a prototypical genus for studying BA deconjugation. We
78 define how the conjugated amino acid moiety drives substrate preferences in distinct BSHs and
79 how those preferences can be leveraged to prevent *C. difficile* spore germination and
80 colonization in pre-clinical models. We further reveal a new function for BSHs, the ability to
81 process an expanded set of substrates including non-canonical conjugated BAs.

82 **Surveying *Lactobacillus* BSH Diversity**

83 To map the range of BSHs harbored by *Lactobacillus*, 3,712 genomes from 274
84 lactobacilli were assembled to comprehensively define the diversity of the enzyme within this
85 key intestinal genus (**Table S1)** (*19*). Highly similar BSH sequence (>95% amino acid identity)
86 were grouped into 84 clusters and a representative sequence from each cluster was used to
87 construct a phylogenetic tree. Nearly all BSH clusters are identified in vertebrate-adapted species
88 and ~40% were human-associated, underscoring their role in host-microbiota symbiosis (**Fig.**
89 **1B, Table S1**).

90 To move toward a functional understanding of BSH activity *in vivo*, 17 diverse
91 BSHs were selected for heterologous expression and purification **(Table S2, Fig. S2)**. BSH
92 activity was screened on a panel of conjugated primary and secondary BAs to comprehensively
93 determine BSH substrate preferences **(Fig. 1C)**. BSHs display a well-defined bias for either
94 glycine or taurine-conjugated BAs. Glycine-preferences dominate the BSHs tested, potentially
95 reflecting the increased abundance of glycine-conjugated BAs among vertebrates (*20*), whereas
96 taurine-specificity is restricted to only a few related BSHs. The glycine-preferring clade
97 containing LaciBSHa, LcriBSHa, and LcriBSHb exhibits the highest activity. Furthermore, the
98 taurine-preferring LaviBSH, LjohBSHc, and LgasBSHa (corresponding to the clusters

99 arrafinosis, johnsonii_1, and gasseri_1, respectively) enzymes are all present within a single
100 major clade while the LsalBSH (cluster salivarius_2) stands alone in a distantly related branch.
101 This suggests that taurine-preference may have evolved twice within *Lactobacillus*. Overall,
102 BSH specialization for glycine or taurine illustrates how lactobacilli may have tailored their
103 metabolism to manage BA exposure.

104 **Structural Basis for BSH Substrate Preference**

105 To dissect the molecular basis of BSH substrate specificity, we determined the
106 crystal structures of six of the *Lactobacillus* BSHs examined above, four glycine-preferring
107 (LgasBSHb, LaciBSHa, LingBSH, LreuBSH) and two taurine-preferring BSHs (LgasBSHa,
108 LjohBSHc; **Fig. 1D, S3A, Table S3**). While most structures were unliganded, LgasBSHa was
109 resolved in complexes with taurine or taurine plus CDCA. All BSHs form tetramers and each
110 monomer exhibits the core four-layered αββα fold typical of the Ntn-hydrolase family (*21*), with
111 RMSD values ranging from 0.5 to 2.0 Å over equivalent Cα positions (**Fig. 2A, S3B**). Within
112 this standard core structure, we noted that each monomer contains a loop donated from a
113 neighboring monomer within the tetramer (**Fig. 2A**). Importantly, sequence analysis revealed
114 that taurine-preferring enzymes contained an S-R-G/S motif in this loop region, while the
115 glycine-preferring enzymes encoded a G-V/T-G motif (**Fig. 2B, Fig. S4**) (*22*). These particular
116 amino acids were also placed directly in each enzyme's active site within the functional BSH
117 tetramers (**Fig. 2C, 2D**). Thus, we hypothesized that these 3-residue motifs play important roles
118 in BSH substrate preferences.

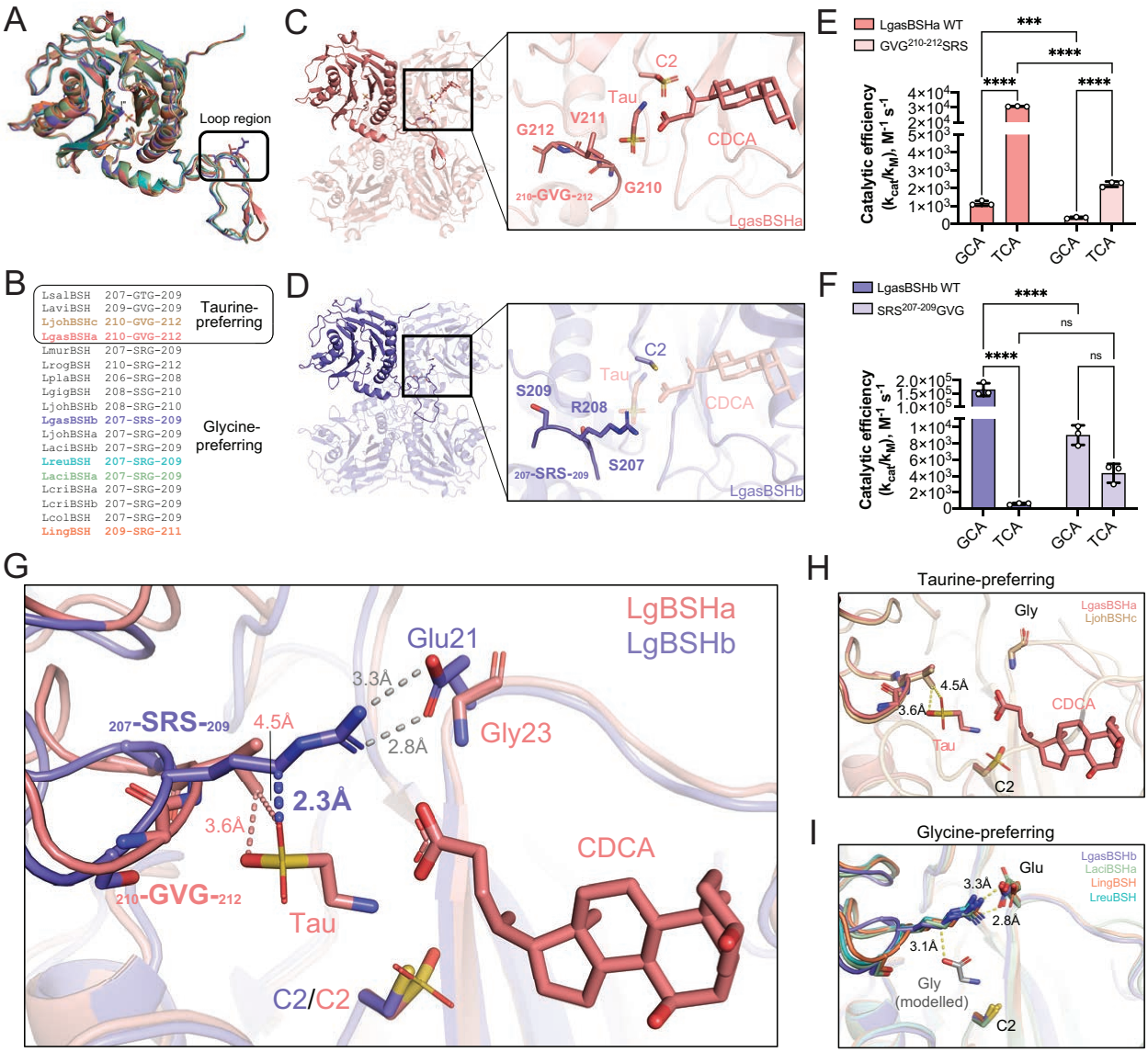

Figure2.

To test this, the 210-GVG-212 region of taurine-preferring LgasBSHa was replaced with SRS, while the 207-SRS-209 region of glycine-preferring LgasBSHb was replaced with GVG, and catalytic efficiencies with conjugates of CA were examined. The LgasBSHa-SRS variant enzyme exhibited significantly reduced catalytic efficiency with TCA, the wild-type enzyme's preferred substrate, while also reducing its processing of GCA (**Fig. 2E**). Similarly, the LgasBSHb-GVG variant showed significantly lower catalytic efficiency with its preferred GCA

127 substrate, and a trend toward increased activity with the non-standard substrate TCA (**Fig. 2F**).
128 Taken together, these functional data support the structure-guided hypothesis that short sequence
129 motifs play important roles in defining the marked glycine *vs.* taurine substrate preferences
130 exhibited by *Lactobacillus* BSHs, reflecting specialization.

131 Structurally, the presence of R208 in LgasBSHb appears to block the processing of
132 taurine-conjugated BAs. When the LgasBSHa and LgasBSHb active sites are overlaid, the
133 distance between LgasBSHb R208 and taurine from the LgasBSHa structure is 2.3 Å, which
134 would generate a steric clash (**Fig. 2G**). In contrast, V211 in LgasBSHa is 3.6 Å away and would
135 not occlude the binding of taurine-conjugated BAs (**Fig. 2G**). Furthermore, R208 in LgasBSHb
136 forms a hydrogen bond with E21 and that interaction creates a more enclosed active site than that
137 seen in taurine preferring BSHs (Fig. 2G). In support of this conclusion, the active sites of the
138 four additional BSH structures resolved here (LjohBSHc, LaciBSHa, LingBSH, LreuBSH)
139 reveal analogous architectures (**Fig. 1D, 2H, I**). Importantly, when a glycine conjugate was
140 modelled into the active site of the glycine-preferring BSHs, the distance between R208 and
141 glycine increased to 3.1 Å, indicating that this smaller substrate can be accommodated with this
142 clade of enzymes (**Fig. 2I**). Together, these data define three-residue motifs as crucial for the
143 glycine vs. taurine conjugate preferences demonstrated by *Lactobacillus* BSHs.

144 **Bile Acids Inhibit *C. difficile* in a Conjugation-Dependent Manner**

145 *C. difficile* infection (CDI) is a significant public health problem that can be
146 difficult to treat with conventional antibiotics (*23*). Even after successful treatment with
147 vancomycin, there remains a high recurrence rate (~30%) (*24*), making a fecal microbiota
148 transplant (FMT) the last line of treatment (*25*). Although FMTs are a lifeline for recurrent CDI
149 (rCDI) patients, the long-term consequences are unknown at this time, making a targeted

150 therapeutic approach urgently needed. Susceptibility to CDI is predominantly driven by
151 antibiotic-driven perturbations to the intestinal microbiota, which results in a loss of colonization
152 resistance (*26, 27*). Strong evidence suggests that microbial BA metabolism is an important
153 mechanism of colonization resistance against *C. difficile* (*28*), as antibiotic usage causes depleted
154 BSHs and increases conjugated BAs (*14*).

155 BAs govern fundamental aspects of *C. difficile*'s pathogenesis: TCA acts as a
156 germinant for *C. difficile* spores (*29*), whereas CDCA can inhibit germination and growth (*30*).
157 Most studies have focused on the production of deconjugated secondary BAs as inhibitors of *C.*
158 *difficile* pathogenesis while few have examined the contributions of BSH activity (*31*). The
159 therapeutic potential of BSHs has been proposed, but gaps in our knowledge of their pleiotropic
160 effects on intestinal biology and their exact mechanism of action have hampered their
161 development (*32, 33*).

162 To determine how BA deconjugation impacts *C. difficile*, we measured the ability
163 of common BAs to inhibit germination in the presence of TCA (**Fig. 3A-C**). Though all BAs
164 tested inhibit germination compared to TCA alone, deconjugated BAs are significantly more
165 inhibitory compared to their taurine-conjugated versions, whereas they are equally or only mildly
166 more inhibitory relative to their glycine-conjugated variants (**Fig 3B**). We also assayed the
167 ability of BAs to inhibit *C. difficile* growth, as we hypothesized that the conjugation would
168 determine BA toxicity (**Fig. 3C**). Taurine-conjugates inhibit growth less while glycine-
169 conjugates and deconjugated BAs are much more toxic. Moreover, taurine-conjugated BAs are
170 significantly less disruptive to *C. difficile*'s membrane integrity compared to glycine-conjugated
171 and deconjugated BAs (**Fig. S5**). Overall, using BSHs to deconjugate taurine-conjugated BAs
172 may be a potent strategy to restrict *C. difficile* in the intestinal tract.

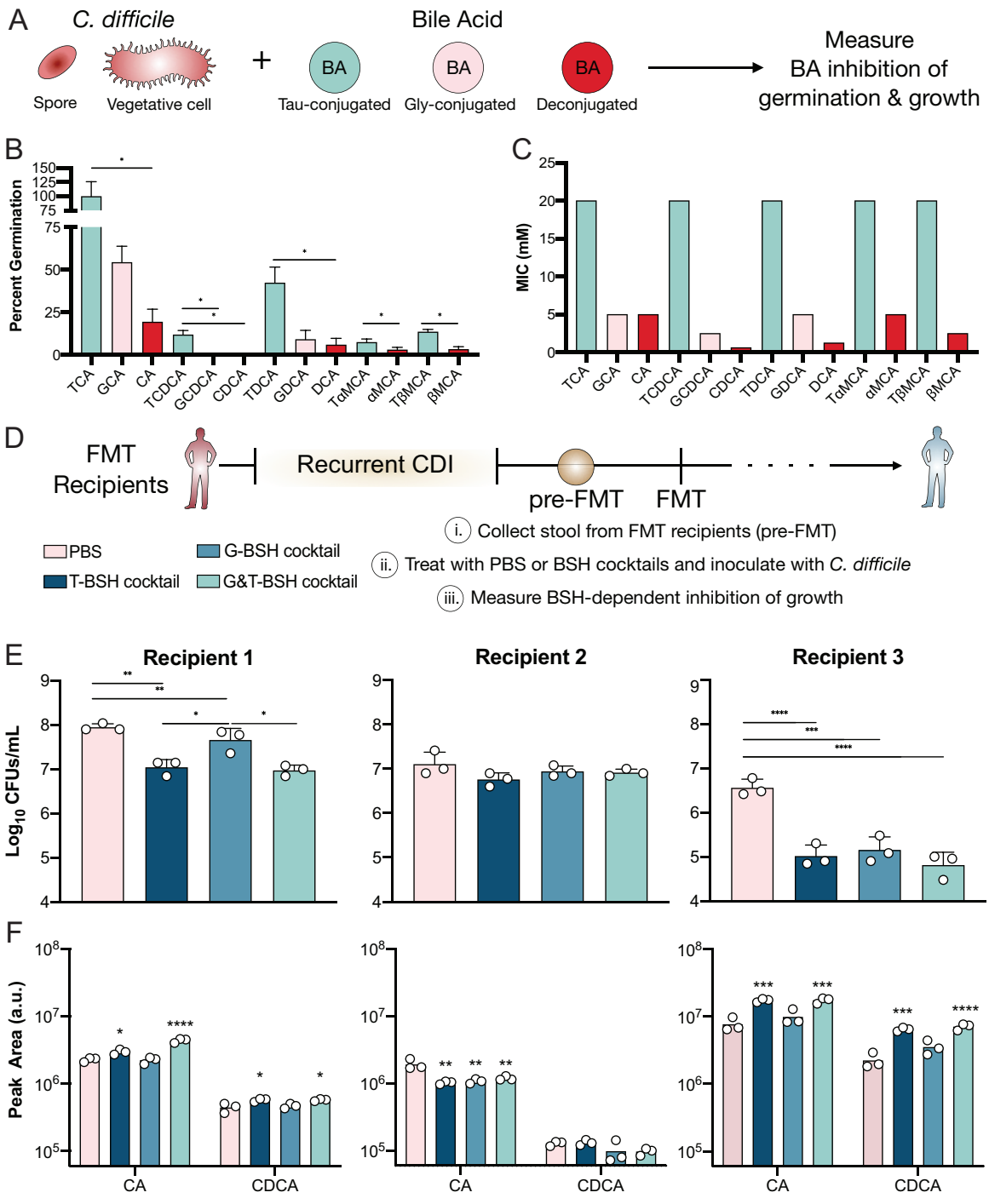

Figure 3.

To determine whether BSHs are sufficient to inhibit *C. difficile* and provide an alternative approach to using antibiotics or FMT, stool from three rCDI patients was collected prior to them receiving an FMT (**Fig 3D**). Unlike mice, FMT recipients have a complex mixture

178 of taurine and glycine-conjugated primary BAs (**Fig S6**). To test whether BSH substrate
179 preference could impact *C. difficile* growth, pre-FMT stool was used to culture *C. difficile* and
180 samples were treated with PBS, a cocktail of taurine-preferring BSHs (T-BSH), glycine-
181 preferring BSHs (G-BSH), or a broadly-acting combination (G&T-BSH) **(Fig. 3E, S7)**. Alone,
182 the BSH cocktails, glycine, or taurine have no impact on *C. difficile* growth (**Fig. S8**). When
183 Recipient 1's stool is treated with the T-BSH and G&T-BSH cocktails, *C. difficile* growth is
184 significantly inhibited at 8 h. Recipient 2's stool doesn't alter *C. difficile* growth when treated
185 with any BSH cocktail, though the T-BSH and G&T-BSH cocktails slightly suppress growth at
186 24 h. Recipient 3's stool robustly suppresses *C. difficile* growth at 8 h using all BSH cocktails,
187 but only the T-BSH and G&T-BSH cocktails maintain that suppression at 24 h.

188 Targeted BA metabolomics was used to assess how the BSH cocktails alter the pre-
189 FMT BA pool and explain the individual variability between recipients (**Fig 3F, S9**). Recipients
190 1 and 3 display an increase in CA and CDCA primarily in response to the T-BSH and G&T-BSH
191 cocktails. Recipient 3's high levels of conjugated BAs prior to BSH treatment explains the BSH
192 cocktail's robust inhibition (**Fig. S6, 9**), Furthermore, Recipient 2 does not display an increase in
193 deconjugated BAs from any BSH treatment, likely due to the overall low concentration of
194 conjugated BAs prior to BSH treatment (**Fig S6**), thereby explaining why no *C. difficile*
195 inhibition was observed in this sample.

196 **BSH Activity Inhibits *C. difficile* Spore Germination and Growth**

197 To interrogate the role of BSHs in colonization resistance against *C. difficile,* we
198 leveraged an antibiotic treated mouse model of CDI, since mice typically have a relatively rich
199 amount of taurine conjugated bile acids. *C. difficile* initiates its infectious cycle when spores
200 arrive and germinate in the small intestine, and then begin to grow and progress to the large

201 intestine where the majority of toxin production and disease occurs. To examine the contribution
202 of BSH activity to colonization resistance along the intestinal tract, we collected murine small
203 intestinal and cecal contents from cefoperazone-treated mice at several times post-antibiotic
204 treatment and supplemented them with PBS or the G&T-BSH cocktail (**Fig. 4A)**. The treated
205 contents were then inoculated with 10^5 spores or CFUs/mL to measure *ex vivo* spore germination
206 and growth, respectively. Remarkably, the addition of the BSH cocktail significantly inhibits *C.*
207 *difficile* spore germination in the small intestinal contents of all mice and suppresses growth at 8
208 and 24 h (**Fig. 4B, C, S10)**. Inhibition of growth is more subtle in the cecum, likely due to the
209 lower concentration of conjugated BAs in this region of the intestinal tract (**Fig. 4D, S11**).
210 Targeted metabolomics was used to corroborate the BSH cocktail's effect on the murine BA
211 pool. Small intestinal samples from day 0 treated with the BSH cocktail display a significant
212 increase in deconjugated BAs (CA, CDCA, βMCA, and UDCA) and a decrease in the taurine-
213 conjugated forms of the same BAs. In the cecum, only CA was significantly deconjugated (**Fig.**
214 **4D, S11**). By day 7 post antibiotic, some mice displayed higher amounts of deconjugated BAs,
215 independent of BSH treatment, coinciding with the return of colonization resistance after
216 antibiotic treatment.

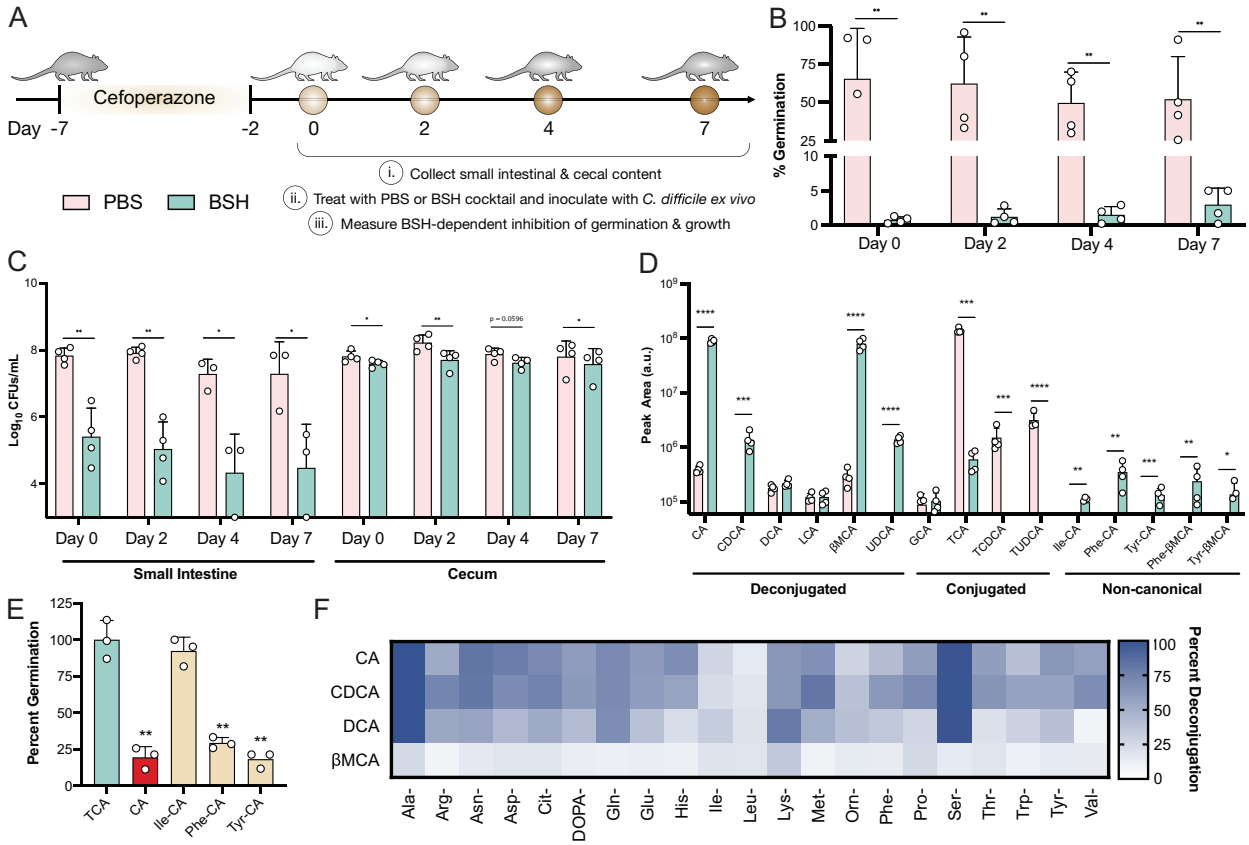

Figure 4

Aside from the increase in deconjugated BAs, the most striking difference in the BA pool is the unexpected increase in non-canonical conjugated BAs in the BSH-treated small intestinal samples (**Fig 4D, S11**). An array of intestinal bacteria can catalyze the conjugation of BAs to a variety of amino acids through an unknown mechanism (**Fig. 1A**) (*16, 17*). Despite their widespread synthesis, there is no evidence at this time that shows that the non-canonical conjugated BAs Ile/Leu-CA, Phe-CA, and Tyr-CA can be deconjugated (*16*). Ile-CA, Phe-CA, and Tyr-CA were among the BAs detected in the small intestinal samples. Given the increased CA and βMCA in the BSH-treated samples, these BAs are likely re-conjugated by the small intestinal microbiota to produce the non-canonical BAs observed. While these BAs did not affect *C. difficile* growth or induce spore germination (**Fig. S12A, B**), Tyr-CA and Phe-CA are able to

229 inhibit spore germination, suggesting for the first time a role for the non-canonical conjugated
230 BAs in colonization resistance against *C. difficile* (**Fig. 4E, S12C**).

231 **BSHs Process Non-Canonical Bile Acids Conjugates**

232 To determine whether BSHs are able to process non-canonical conjugated BAs, we
233 screened a larger range of BSHs and BAs (**Fig. S13**). While activity with these non-canonical
234 conjugates was low compared to the canonical conjugations, some BSHs, like LingBSH and
235 LreuBSH, exhibit appreciable activity on non-canonical BAs. To understand the recalcitrance of
236 non-canonical conjugated BAs, we broadly monitored the deconjugation of 5 BSHs (LingBSH,
237 LgasBSHa, LgasBSHb, LjohBSHc, and LreuBSH) with assorted preferences (**Fig. S14A**). BSHs
238 were incubated with non-canonical conjugated BAs pools (AA-CA, AA-CDCA, AA-DCA, and
239 AA- βMCA) that consist of one BA (CA, CDCA, DCA, or βMCA) conjugated to 22 different
240 amino acids, excluding taurine and glycine (*18*), and initial BA deconjugation was quantified
241 using LC-IMS-MS (**Fig. S14B**). LingBSH displays exceptional activity, suggesting that some
242 BSHs may be uniquely adapted to process this expanded repertoire of BAs (**Fig. 4F, 14B, S15**).
243 Ala and Ser-conjugated BAs are efficiently processed, and these observations were validated
244 using purified Ala-CA and Ser-CA demonstrating that their susceptibility to deconjugation is
245 similar to GCA and TCA (**Fig. S13**). Ala and Ser are the smallest amino acids next to Gly,
246 suggesting that the steric constraints of the active site could dictate non-canonical conjugate
247 deconjugation (**Fig. S15, S16)**. Notably, amine-containing amino acids such as Lys, Gln, and
248 Asn are enriched and among the most efficiently processed conjugates (**Fig. S16**).

249 We also examine whether non-canonical conjugated BA processing would occur in
250 BSH-expressing *L. gasseri* cells. Wild-type, Δ*bshA*, Δ*bshB*, and Δ*bshAB L. gasseri* was grown
251 and reacted with the AA-CDCA pool and supernatants were used to detect deconjugation.

252 Δ*bshAB* displayed some deconjugation, possibly due to cells sequestering BAs (**Fig. S14C)**.
253 Individual BSH activities and substrate preferences were comparably maintained *in vivo*,
254 demonstrating that BSH-expressing bacteria are capable of non-canonical BA deconjugation, and
255 that they do so based on the enzymatic preferences of the BSHs they encode.
256
257 **Discussion**
258 There is a growing appreciation for the roles that BSH substrate preferences play in
259 the management of disease (*6, 8*). This work stresses the distinction between the deconjugation
260 of glycine and taurine-conjugated BAs, the latter of which has been shown to play a role in the
261 establishment of colonization resistance against *Klebsiella pneumoniae* and the development of
262 colorectal cancer (*34, 35*). Our analysis of *C. difficile*-BA sensitivities motivated the use of
263 glycine and taurine-preferring *Lactobacillus* BSHs to optimally inhibit *C. difficile ex vivo* (**Fig.**
264 **3D**). Thus, leveraging BA metabolism to restore colonization resistance may be an alternative
265 therapy that avoids antibiotic damage, the unspecified risks of FMTs, and the variability of live
266 biotherapeutics.
267 The extensive variety of recently identified non-canonical conjugated BAs expands
268 the complexity of the BSH-BA pool and reinforces BSHs as key BA-altering enzymes (*16, 17*).
269 BSH-generated deconjugated BAs fuel the production of non-canonical conjugated BAs (**Fig.**
270 **4D**). While the mechanism and purpose of this re-conjugation is yet to be elucidated, our
271 observation that non-canonical conjugations can inhibit *C. difficile* spore germination introduces
272 new mechanistic avenues by which BSH activity can be used to restore colonization resistance
273 (**Fig. 4E**). We also demonstrate that BSHs can variably act on these BAs to support a model
274 where BSHs directly shape the non-canonical conjugated BA pool by simultaneously sustaining

275 and curtailing it (**Fig. 4D, S14**). Given the broad impacts BSH can have on the overall BA pool,
276 purposefully augmenting the specificity or activity of BSHs could support their potential use as a
277 precision modality to steer BA metabolism *in vivo*.

278 BSHs perform the important role of BA deconjugation, and perturbations to this
279 process are implicated in several diseases including CDI. *C. difficile* pathogenesis is
280 exceptionally responsive to alterations in BSH activity, thereby establishing these enzymes as a
281 potential targeted approach to restore colonization resistance. The preferences and efficiency by
282 which BSHs recognize conjugated BAs defines the resulting BA pool, and their ability to
283 variably process the expansive catalogue of non-canonical conjugated BAs is a newly prescribed
284 function of BSHs. In the future, BSHs may be leveraged to rationally manipulate the chemical
285 complexity of the BA pool toward addressing many states of intestinal disease.

286 **References**

287 1. M. H. Foley, S. O'Flaherty, R. Barrangou, C. M. Theriot, Bile salt hydrolases:
288 Gatekeepers of bile acid metabolism and host-microbiome crosstalk in the
289 gastrointestinal tract. *PLoS Pathog* **15**, e1007581 (2019).

290 2. C. L. Gentile, T. L. Weir, The gut microbiota at the intersection of diet and human health.
291 *Science* **362**, 776-780 (2018).

292 3. A. Lavelle, H. Sokol, Gut microbiota-derived metabolites as key actors in inflammatory
293 bowel disease. *Nat Rev Gastroenterol Hepatol* **17**, 223-237 (2020).

294 4. S. N. Chaudhari *et al.*, Bariatric surgery reveals a gut-restricted TGR5 agonist with anti-
295 diabetic effects. *Nat Chem Biol* **17**, 20-29 (2021).

296 5. K. Govindarajan *et al.*, Unconjugated bile acids influence expression of circadian genes:
297 A potential mechanism for microbe-host crosstalk. *PLoS One* **11**, e0167319 (2016).

298 6. L. Yao *et al.*, A selective gut bacterial bile salt hydrolase alters host metabolism. *Elife* **7**,
299 (2018).

300 7. K. B. Islam *et al.*, Bile acid is a host factor that regulates the composition of the cecal
301 microbiota in rats. *Gastroenterology* **141**, 1773-1781 (2011).

302 8. M. H. Foley *et al.*, *Lactobacillus* bile salt hydrolase substrate specificity governs bacterial
303 fitness and host colonization. *Proc Natl Acad Sci U S A* **118**, (2021).

304 9. J. M. Ridlon, S. C. Harris, S. Bhowmik, D. J. Kang, P. B. Hylemon, Consequences of bile
305 salt biotransformations by intestinal bacteria. *Gut Microbes* **7**, 22-39 (2016).

306 10. B. Jia, D. Park, Y. Hahn, C. O. Jeon, Metagenomic analysis of the human microbiome
307 reveals the association between the abundance of gut bile salt hydrolases and host health.
308 *Gut Microbes* **11**, 1300-1313 (2020).

309 11. J. M. Ridlon, D. J. Kang, P. B. Hylemon, Bile salt biotransformations by human intestinal
310 bacteria. *J Lipid Res* **47**, 241-259 (2006).
311 12. S. A. Joyce *et al.*, Regulation of host weight gain and lipid metabolism by bacterial bile
312 acid modification in the gut. *Proc Natl Acad Sci U S A* **111**, 7421-7426 (2014).
313 13. C. Ma *et al.*, Gut microbiome-mediated bile acid metabolism regulates liver cancer via
314 NKT cells. *Science* **360**, (2018).
315 14. C. M. Theriot *et al.*, Antibiotic-induced shifts in the mouse gut microbiome and
316 metabolome increase susceptibility to *Clostridium difficile* infection. *Nat Commun* **5**,
317 3114 (2014).
318 15. B. H. Mullish *et al.*, Microbial bile salt hydrolases mediate the efficacy of faecal
319 microbiota transplant in the treatment of recurrent *Clostridioides difficile* infection. *Gut*
320 **68**, 1791-1800 (2019).
321 16. R. A. Quinn *et al.*, Global chemical effects of the microbiome include new bile-acid
322 conjugations. *Nature* **579**, 123-129 (2020).
323 17. L. N. Lucas *et al.*, Dominant bacterial phyla from the human gut show widespread ability
324 to transform and conjugate bile acids. *mSystems*, e0080521 (2021).
325 18. E. Gentry *et al.*, https://www.researchsquare.com/article/rs-820302/v1. *Nature Portfolio*,
326 (2022).
327 19. S. O'Flaherty, A. Briner Crawley, C. M. Theriot, R. Barrangou, The *Lactobacillus* bile
328 salt hydrolase repertoire reveals niche-specific adaptation. *mSphere* **3**, (2018).
329 20. G. A. Nagana Gowda, N. Shanaiah, A. Cooper, M. Maluccio, D. Raftery, Bile acids
330 conjugation in human bile is not random: new insights from (1)H-NMR spectroscopy at
331 800 MHz. *Lipids* **44**, 527-535 (2009).

332 21. F. Xu *et al.*, The complex structure of bile salt hydrolase from *Lactobacillus salivarius*
333 reveals the structural basis of substrate specificity. *Sci Rep* **9**, 12438 (2019).
334 22. F. Madeira *et al.*, The EMBL-EBI search and sequence analysis tools APIs in 2019.
335 *Nucleic Acids Res* **47**, W636-W641 (2019).
336 23. C. Slimings, T. V. Riley, Antibiotics and hospital-acquired *Clostridium difficile* infection:
337 update of systematic review and meta-analysis. *J Antimicrob Chemother* **69**, 881-891
338 (2014).
339 24. O. A. Cornely, M. A. Miller, T. J. Louie, D. W. Crook, S. L. Gorbach, Treatment of first
340 recurrence of *Clostridium difficile* infection: fidaxomicin versus vancomycin. *Clin Infect*
341 *Dis* **55 Suppl 2**, S154-161 (2012).
342 25. C. R. Kelly *et al.*, Effect of fecal microbiota transplantation on recurrence in multiply
343 recurrent *Clostridium difficile* infection: A randomized trial. *Ann Intern Med* **165**, 609-
344 616 (2016).
345 26. R. C. Owens, Jr., C. J. Donskey, R. P. Gaynes, V. G. Loo, C. A. Muto, Antimicrobial-
346 associated risk factors for *Clostridium difficile* infection. *Clin Infect Dis* **46 Suppl 1**, S19-
347 31 (2008).
348 27. R. A. Britton, V. B. Young, Role of the intestinal microbiota in resistance to colonization
349 by *Clostridium difficile*. *Gastroenterology* **146**, 1547-1553 (2014).
350 28. A. D. Reed, C. M. Theriot, Contribution of nhibitory metabolites and competition for
351 nutrients to colonization resistance against *Clostridioides difficile* by Commensal
352 Clostridium. *Microorganisms* **9**, (2021).
353 29. J. A. Sorg, A. L. Sonenshein, Bile salts and glycine as cogerminants for *Clostridium*
354 *difficile* spores. *J Bacteriol* **190**, 2505-2512 (2008).

355 30. J. A. Sorg, A. L. Sonenshein, Chenodeoxycholate is an inhibitor of *Clostridium difficile*
356 spore germination. *J Bacteriol* **191**, 1115-1117 (2009).
357 31. R. Thanissery, J. A. Winston, C. M. Theriot, Inhibition of spore germination, growth, and
358 toxin activity of clinically relevant *C. difficile* strains by gut microbiota derived
359 secondary bile acids. *Anaerobe* **45**, 86-100 (2017).
360 32. M. L. Jones, C. Tomaro-Duchesneau, C. J. Martoni, S. Prakash, Cholesterol lowering
361 with bile salt hydrolase-active probiotic bacteria, mechanism of action, clinical evidence,
362 and future direction for heart health applications. *Expert Opin Biol Ther* **13**, 631-642
363 (2013).
364 33. S. A. Joyce, F. Shanahan, C. Hill, C. G. Gahan, Bacterial bile salt hydrolase in host
365 metabolism: Potential for influencing gastrointestinal microbe-host crosstalk. *Gut*
366 *Microbes* **5**, 669-674 (2014).
367 34. A. Stacy *et al.*, Infection trains the host for microbiota-enhanced resistance to pathogens.
368 *Cell* **184**, 615-627 e617 (2021).
369 35. J. M. Ridlon, P. G. Wolf, H. R. Gaskins, Taurocholic acid metabolism by gut microbes
370 and colon cancer. *Gut Microbes* **7**, 201-215 (2016).
371 36. R. M. Duar *et al.*, Lifestyles in transition: evolution and natural history of the genus
372 *Lactobacillus*. *FEMS Microbiol Rev* **41**, S27-S48 (2017).
373
374 **Acknowledgements:** This work was performed in part by the Molecular Education, Technology
375 and Research Innovation Center (METRIC) at NC State University, which is supported by the
376 State of North Carolina.
377 **Funding:** We thank IFF for supporting this study. MHF was supported by the University of
378 North Carolina Center for Gastrointestinal Biology and Disease postdoctoral fellowship training

379 grant T32DK07737. MEW was supported through the NIH training grant T32GM008570 and
380 NSF DGE-1650116. This study was also supported by the NIGMS R35 GM119438, and R01
381 GM135218 and GM137286; NIEHS P30 ES025128, P42 ES027704, and P42 ES031009; and the
382 Environmental Protection Agency STAR RD 84003201 award. The FMT study was supported
383 by the NCTraCS Translational and Clinical Sciences Institute Pilot Grant UNCSUR11609. MD
384 was supported by NIH training grant T32 DK007634.

385 **Author contributions:** MHF, MEW, SOF, ECP, MRR, RB, CMT designed the research. MHF,
386 MEW, AKS, SOF, ECG, GA, SP, MP, VVB, MEV, and ESB performed, analyzed, and
387 interpreted experiments. SOF and MP performed bioinformatic analysis of BSHs. MHF and GA
388 performed all BSH specific activity assays and *C. difficile* experiments. MEW, SP, and VVB
389 performed crystallographic work. MD, SKM, and AJ collected patient samples. AKS performed
390 metabolomic analyses. ECG synthesized non-canonical bile acids. MF and MEW wrote the
391 manuscript which all authors edited.

392 **Competing interests:** MRR is a Founder of Symberix, Inc., which is developing microbiome-
393 targeted therapeutics. MRR is also the recipient of research funding from Merck and Lilly,
394 although those funds were not used in this project. PCD is a scientific advisor to Cybele and is a
395 co-founder and scientific founder of Ometa and Enveda, with prior approval by UC-San Diego.
396 CMT consults for Vedanta Biosciences, Inc. and Summit Therapeutics. CMT is a founder of
397 CRISPR Biotechnologies. RB is a founder of Ancilia Bioscience and CRISPR Biotechnologies.
398 MHF, SOF, RB and CMT are inventors on a patent application related to the use of
399 *Lactobacillus* BSH enzymes

400 **Data and materials availability:** All data associated with this study are available in the main
401 text or the Supplementary Materials. All LC-IMS-MS data are publicly available on Panorama

402 under the Panorama dashboard of the Baker Lab-NCSU within the “0821 BSH Assessment”,

403 “1121 Mouse Germination and Growth Ex-Vivo” and the “1121 Theriot FMT Ex-Vivo Growth”

404 projects."

405 **List of Supplementary materials:**

406 Materials and Methods

407 Fig S1 to S17

408 Table S1 to S3

409 **Figure legends**

410 **Figure 1. *Lactobacillus* BSHs have distinct substrate preferences.**

411 (A) Overview of BA metabolism using cholic acid (CA) as an example. BAs are synthesized and
412 conjugated with a taurine or glycine (T/GCA) by the liver enzyme Baat. Conjugated BAs are
413 deconjugated by BSHs, allowing transformations such as 7α-dehydroxylation encoded by the *bai*
414 operon to generate secondary BAs like DCA. Deconjugated BAs can be re-conjugated to
415 produce non-canonical conjugated BAs like Tyr-CA. (B) The *Lactobacillus* BSH phylogenetic
416 tree was assembled from 84 BSH clusters. Major clades are distinguished by branch color. Each
417 cluster name indicates the BSH-encoding species with the inner metadata layers indicating
418 lifestyle and isolation source (*36*). The outer metadata layer indicates the BSHs cloned for
419 characterization with diamonds indicating BSH crystal structures presented here. (C) Heatmap of
420 BSH activity across conjugated BAs. The clade highlighted in blue displays preference for
421 taurine-conjugated BAs. Values represent mean specific activity (n = 3-4). Phylogenetic
422 relationships between BSHs are based on amino acid sequences. (D) Superposition of the
423 taurine- and glycine-preferring BSH enzyme tetramer crystal structures presented here.

424 **Figure 2. BSH loop region dictates enzyme substrate preference.**

425 (A) Superimposed monomers of the six BSH monomer structures presented here highlighting the
426 substrate preference loop and colored as indicated in panel B. (B) Sequence alignment of the
427 loop region of *Lactobacillus* BSHs. Resolved structures are colored as indicated, with a constant

428 coloring scheme throughout the figure. Taurine-preferring enzymes exhibit a G-V/T-G motif,
429 while glycine-preferring enzymes maintain a S-R-G/S motif. (C) The LgasBSHa tetramer with
430 the active site shown in the inset, with the catalytic cysteine at position 2, the bound taurine and
431 CDCA compounds, and the GVG swapped into the active site from the neighboring monomer
432 highlighted. (D) The LgasBSHb tetramer with the active site shown in the inset, with the
433 catalytic cysteine at position 2 and the SRS swapped into the active site from the neighboring
434 monomer highlighted. The taurine and CDCA ligands from the LgasBSHa structure are also
435 rendered transparently. (E, F) Catalytic efficiency for wild-type and mutant forms of LgasBSHa
436 and LgasBSHb with GCA and TCA. Bars are the average of n=3 ± standard deviation.
437 Significant differences were tested by two-way ANOVA with Tukey's multiple comparisons test
438 (ns not significant, ***$p < 0.001$, ****$p < 0.0001$). (G) Superposition of the active sites of
439 LgasBSHa and LgasBSHb showing that taurine is accommodated by Val211 of LgasBSHa but
440 clashes at 2.3 Å with the side chain of Arg208 in LgasBSHb, which is held in place via a salt
441 bridge with Glu21. (H, I) Superpositions of the active sites of the two taurine-preferring or the
442 four glycine-preferring BSH structures presented here reveals consistent active site architectures
443 that accommodate taurine or glycine, respectively.
444 **Figure 3. Deconjugated BAs and BSH activity can inhibit *C. difficile*.** (A) Schematic of *in*
445 *vitro* BA-dependent inhibition of *C. difficile* germination and growth. (B) Inhibition of spore
446 germination using various BAs (0.75 mM) with the germinant TCA (2 mM). (C) Inhibition of *C.*
447 *difficile* growth as determined by minimum inhibitory concentration (MIC) testing. Statistical
448 differences in B and C were assessed by a one-tailed Welch's *t* test. (D) Schematic of pre-FMT
449 collection and *ex vivo* growth. Pre-FMT stool collected from rCDI patient was supplemented
450 with PBS or a BSH cocktail and subsequently inoculated with *C. difficile*. (E) *C. difficile* growth

451 was measured at 8h. (F) Targeted metabolomics showing the deconjugated BAs CA and CDCA
452 from the samples from E. Statistical differences tested by one-way repeated measures ANOVA
453 with Sidak's correction for multiple comparisons. All bars represent the average of n=3
454 replicates ± sd. *$p < 0.05$, **$p < 0.01$, ***$p < 0.001$, ****$p < 0.0001$.

455 **Figure 4. BSHs shape the non-canonical conjugated BA pool that governs *C. difficile* spore**
456 **germination** (A) Schematic of BSH-dependent inhibition of *ex vivo C. difficile* germination and
457 growth. Intestinal contents harvested from cefoperazone-treated mice (n = 3-4) were
458 supplemented with a cocktail of BSHs and then inoculated with *C. difficile* spores or cells to
459 measure germination or growth, respectively. (B) Germination of *C. difficile* spores in murine
460 small intestinal contents. Contents were treated for 8h with PBS or a BSH cocktail before
461 inoculation. (C) Growth at 8h of *C. difficile* in murine intestinal contents. Contents were treated
462 with PBS or a BSH cocktail and inoculated simultaneously. Statistical differences were tested by
463 ratio paired *t* test. (D) Targeted metabolomics showing the BAs identified in the Day 0 small
464 intestinal samples from C. (E) Inhibition of *C. difficile* germination using various BAs (0.75
465 mM) with the germinant TCA (2 mM). Statistical differences were assessed by one-tailed *t* test.
466 Bars represent mean ± standard deviation. (F) Heatmap of LingBSH across all non-canonical BA
467 pools. Values represent the mean from n = 3 replicates of % deconjugation after 5 minutes. Bars
468 represent mean of n=3-4 ± standard deviation. *$p < 0.05$, **$p < 0.01$, ***$p < 0.001$, ****$p <$
469 0.0001.